
NONLINEAR WAVE STRUCTURES IN COMPLEX PLASMAS: THEORY AND EXPERIMENTS

S.I. POPEL, G.E. MORFILL¹

UDC 533.9

© 2005

Institute for Dynamics of Geospheres, Russian Acad. Sci.
(38-1, Leninsky Prosp., Moscow 119334, Russia; e-mail: s-i.popel@mtu-net.ru),

¹Centre for Interdisciplinary Plasma Science,
Max-Planck-Institut für Extraterrestrische Physik
(Garching D-85740, Germany)

Theoretical and experimental results on nonlinear wave structures in complex (dusty) plasmas are reviewed. It is shown that the hydrodynamic ionization source model is applicable to the nonlinear dust ion-acoustic structures in a double plasma device and a Q-machine device. The most important dissipative processes which are responsible for the generation of dust ion-acoustic nonlinear structures are investigated. Among them are the anomalous dissipation due to dust charging process, absorption and scattering of ions by dust grains, as well as the kinetic (including Landau) damping. Possibilities of observation of the dust ion-acoustic shocks in active rocket experiments in Earth's ionosphere as well as applications of such shocks to natural phenomena and technologies are discussed. Dust acoustic nonlinear structures are described both in strongly and weakly coupled complex plasmas.

Introduction

A complex (dusty) plasma is the plasma containing electrons, ions, neutrals, and dust microscopic particles which are composed of either solid or liquid material [1–6]. It is always an open system because the currents of electrons and ions flowing onto dust grains (as well as the energy flows) should be maintained by external sources of the plasma particles and the energy. The dissipation rate is high. Therefore, there is a tendency to the self-organization and to the formation of long-living nonlinear dissipative and coherent structures in a plasma such as shock waves, solitons, cavitons, collapsing cavities, etc. One can expect wider manifestations of nonlinear structures in complex plasmas than in the case of usual plasmas. The significant property of complex plasmas is the dust particle charging process. As a rule, under conditions of laboratory experiments the microparticles are negatively charged, their charges being determined by the fluxes of electrons and ions, which are absorbed by microparticles. Any changes of plasma parameters vary these fluxes that results in a variable charge of the latter.

At present, the problem of the excitation and propagation of nonlinear perturbations occupies an important place in the physics of complex plasma. Interest in this kind of research is often associated with the fact that the processes of dust grain charging are far from equilibrium, so that the anomalous dissipation, which, by its very nature, originates from the charging process, can play a decisive role [7]. It is this anomalous dissipation mechanism that is responsible for the existence of a new kind of shocks [8], namely dust ion-acoustic shocks, that are “collisionless” in the sense that they are almost completely insensitive to electron-ion collisions. However, in contrast to classical collisionless shock waves, the dissipation due to dust charging involves the interaction of electrons and ions with dust grains through microscopic electron and ion currents to the grain surfaces. The anomalous dissipation plays a very important role in the propagation of other dust ion-acoustic nonlinear structures, e.g., in the case of the so-called “weakly dissipative” dust ion-acoustic solitons [9], whose shape is described by soliton solutions in a certain range of values of the Mach number. Because of the anomalous dissipation, these solitons are slowed down and damped.

Dust ion-acoustic shock waves were observed in a double plasma device at the Institute of Space and Astronautical Science (Japan) [10] and in a Q-machine device at the University of Iowa (USA) [11] almost simultaneously. The observation of dust ion-acoustic solitons was reported in [12].

Experiments on shock waves in complex plasmas are conducted in a number of major research laboratories throughout the world. In particular, in strongly coupled complex plasmas, Mach cone shocks were reported [13, 14]. The experimental observation of a shock wave of sufficient strength to melt a two-dimensional plasma crystal, through which it propagates, was presented in [15]. A large-amplitude dust wave with two humps of dust density, separated by a dip, was generated in a dc

glow-discharge plasma [16]. Dust acoustic shocks were observed in a microgravity experiment on the board of the International Space Station [17]. There are also plans to carry out experiments on dust ion-acoustic shock waves during the mission of the International Space Station.

The purpose of this brief review is to present the most important results on nonlinear wave structures in complex plasmas.

1. Dust Ion-Acoustic Shocks in Laboratory Plasmas

Let us formulate the main experimental results on dust ion-acoustic shocks in complex plasmas. In experiments [10], Nakamura et al. revealed that the most important feature of dust ion-acoustic shocks in complex plasmas is the following.

(i) In the absence of dust, the effect of the electron and ion charge separation gives rise to oscillations in the shock wave profile in the vicinity of the shock front, while the presence of dust suppresses these oscillations.

The experiments [11] showed that:

(ii) Dust ion-acoustic shocks are generated at sufficiently high dust densities (under the experimental conditions of [11], at dust densities such that $\epsilon Z_{d0} \equiv n_{d0} Z_{d0} / n_{i0} \geq 0.75$, where $q_d = -Z_d e$ is the dust grain charge, $-e$ is the electron charge, $n_{d(i)}$ is the dust (ion) density, and the subscript "0" stands for the unperturbed plasma parameters). In [11], the conclusion about the formation of a shock wave was drawn from the fact that the perturbation front steepens as time elapses. At sufficiently low dust densities, the perturbation front does not steepen but instead widens.

(iii) When the shock wave structure has formed, the shock front width $\Delta\xi$ is described by the theoretical estimate which is based on the model developed in [8]:

$$\Delta\xi \sim M c_s / \nu_q, \quad (1)$$

Here, $M c_s$ is the shock wave speed, M is the Mach number, $c_s = \sqrt{T_e / m_i}$ is the ion-acoustic speed, $\nu_q = \omega_{pi}^2 a (1 + z_0 + T_i / T_e) / \sqrt{2\pi} \nu_{Ti}$ is the grain charging rate, $\omega_{pi} = \sqrt{4\pi n_{i0} e^2 / m_i}$ is the ion plasma frequency, m_i is the ion mass, a is the dust grain radius, $z = Z_d e^2 / a T_e$, $T_{e(i)}$ is the electron (ion) temperature, and $\nu_{Ti} = \sqrt{T_i / m_i}$ is the ion thermal velocity.

(iv) The velocity of the dust ion-acoustic shocks increases considerably with increasing ϵZ_{d0} .

In this context, the requirement to a theoretical model is the adequate description of relevant

experiments. We use the so-called ionization source model developed in [18, 19] and based on the hydrodynamic approach. We note that, under the experimental conditions of [10, 11], the ionization source term in the evolutionary equation for the ion density should be independent of the electron density.

Now, we test our theoretical model against the experimental result (i) which was obtained in [10]. The experiments described in that paper were carried out with a double plasma device which was modified so that the dust component was present in the plasma. The parameters of the dusty plasma were as follows: $T_e \approx 1 \div 1.5$ eV, $T_i < 0.1$ eV, the unperturbed electron density $n_{e0} \sim 10^8 \div 10^9$ cm⁻³, and the dust grain radius $a \approx 4.4$ μ m. The unperturbed dust density n_{d0} was varied from 0 to about 10^5 cm⁻³. Dust ion-acoustic shock waves were excited by applying a triangular voltage pulse with a peak amplitude of 2.0 V and a rise time of about μ s to the driver anode. The calculations were carried out for different dust densities and for the following parameter values: $T_e = T_i = 1.5$ eV, $n_{i0} = 2.3 \times 10^8$ cm⁻³ (the ion background density was the same for all series of simulations), and the dust grain radius $a = 4.4$ μ m. The width of the perturbation ($\Delta x \approx 20$ cm) and its shape were determined self-consistently, in accordance with the method for exciting a shock wave. It should be noted that Nakamura and Bailung [20] compared the theoretical and experimental potential differences between the grains and the plasma under essentially the same conditions as those prevailing in the experiments of [10]. They found that, although the ion temperature in those experiments was significantly lower than the electron temperature ($T_i \ll T_e$), the experimental results were best fitted by the curve calculated for $T_i = T_e$. They attributed this circumstance to the possible ion acceleration to energies comparable to the electron energy. That is why, in our calculations, the values of the electron and ion temperatures were taken to be the same. In Fig. 1 (which is analogous to Fig. 3 from [10]), we illustrate the time evolution of the ion density at different distances from the grid. The time evolutions were calculated for (a) $n_{d0} = 0$ (the electron density being $n_{e0} = 2.3 \times 10^8$ cm⁻³) and (b) $n_{d0} = 1.46 \times 10^4$ cm⁻³ (the electron density being $n_{e0} = 4.6 \times 10^8$ cm⁻³). We can see that the electron and ion charge separation gives rise to oscillations in the shock wave profile and that the dust suppresses these oscillations, as is the case in the experiments of [10]. The theoretically calculated rise time of the shock front is about 5 μ s, which corresponds to the experimental data.

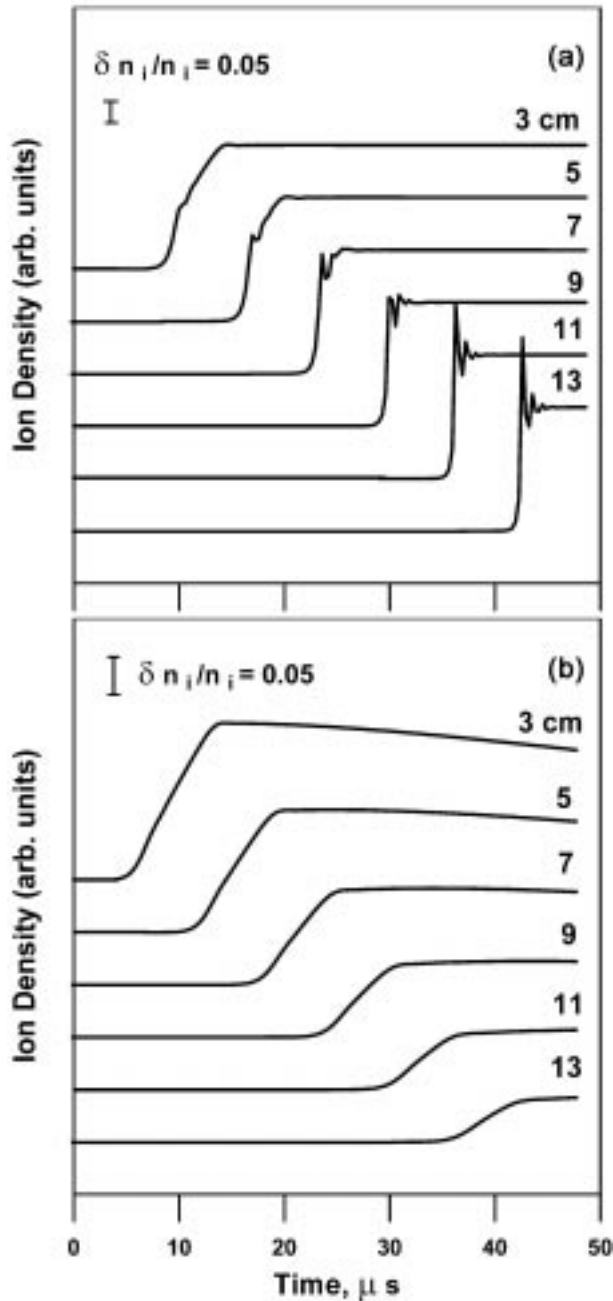


Fig. 1. Time evolutions of the ion density at different distances from the grid for two different values of the dust density: $n_{d0} = 0$ (a) and $n_{d0} = 1.46 \times 10^4 \text{ cm}^{-3}$ (b). The remaining dusty plasma parameters are $T_e = T_i = 1.5 \text{ eV}$, $n_{i0} = 2.3 \times 10^8 \text{ cm}^{-3}$, and $a = 4.4 \mu\text{m}$. Like in the experiment of [10], the oscillations in the shock wave profile due to the separation of charges (electrons and ions) are suppressed by the dust

The modeling of the experiments [11] performed with a Q-machine has been carried out for the following values

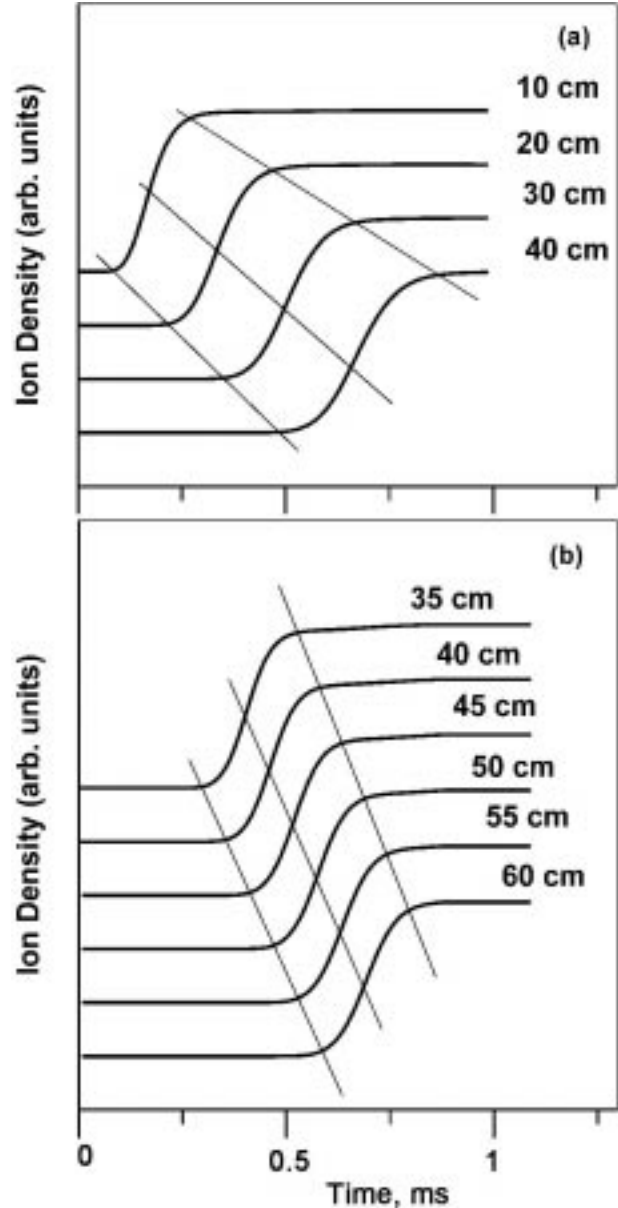


Fig. 2. Time evolutions of the ion density (heavy curves) at different distances from the grid for $\epsilon Z_{d0} = 0$ (a) and $\epsilon Z_{d0} = 0.75$ (b). The remaining parameters of the dusty plasma and of the perturbation are as follows: $T_e = T_i = 0.2 \text{ eV}$, $n_{i0} = 1.024 \times 10^7 \text{ cm}^{-3}$, $a = 0.1 \mu\text{m}$, $\Delta x = 25 \text{ cm}$, and $\Delta n_i/n_{i0} = 2$. The light lines show the widening of the wave front (at $\epsilon Z_{d0} = 0$) and its steepening (at $\epsilon Z_{d0} = 0.75$), which agrees with the experimental data of [11]

of cesium vapor plasma parameters, which correspond to the experimental ones: the electron and ion temperatures were equal to one another, $T_e = T_i = 0.2 \text{ eV}$; the

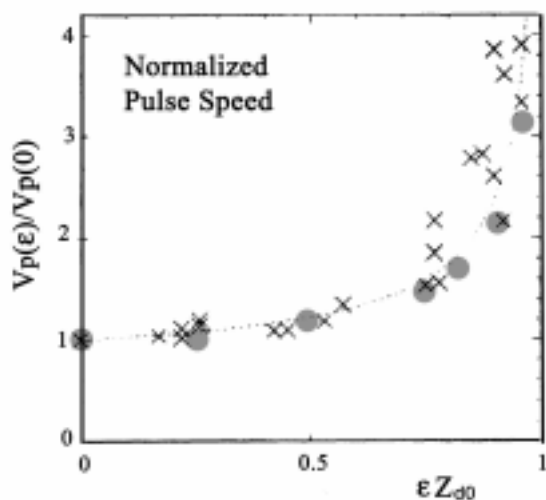


Fig. 3. Dependence of the perturbation front velocity (normalized to its value in the absence of dust) on ϵZ_{d0} . The crosses refer to the experimental points obtained in [11] and the calculated results are represented by the closed circles

background ion density $n_{i0} = 1.024 \times 10^7 \text{ cm}^{-3}$ was the same for all series of simulations; the grain radius was $a = 0.1 \text{ } \mu\text{m}$; the width of the rectangular initial perturbation, which is created in the Q-machine with the aid of a grid preventing most of the plasma from passing through, was 25 cm; and the excess initial perturbed ion density above the background ion density in the remaining unperturbed plasma was $\Delta n_i/n_{i0} = 2$ (see Fig. 2 in [11]). The grid is normally biased at about -6 V with respect to the grounded hot plate and absorbs a large fraction of the ions impinging on it. By suddenly changing the bias to about -2 V (\sim the plasma space potential), the grid “opens up”, launching a large amplitude density pulse downstream toward the end plate (right border of the Q-machine).

The calculations were carried out for different values of the parameter ϵZ_{d0} . In Fig. 2 (which is analogous to Fig. 2 from [11]), we illustrate the time evolution of the ion density at different distances from the grid. The time evolutions (heavy curves) were calculated for $\epsilon Z_{d0} = 0$ (a) and $\epsilon Z_{d0} = 0.75$ (b). The light curves show the widening of the wave front (at $\epsilon Z_{d0} = 0$) and its steepening (at $\epsilon Z_{d0} = 0.75$). This agrees with the experimental data from [11].

The extent to which the shock front widens was calculated to be $\Delta\xi/Mc_s \sim 0.3 \text{ ms}$ (see Fig. 2,b), which corresponds to that observed experimentally (see Fig. 2,b in [11]) and also to the estimate obtained using the theoretical model of [8].

In the data shown in Fig. 2,b in [11], we notice that in the case where dust is present, the amplitude of the shock decreases as we move away from the grid. Such a decrease in the shock amplitude is due to momentum loss by ions as a result of their absorption on the grain surfaces and their Coulomb collisions with grains and is associated, in particular, with an attenuation of the ion flux as ions pass through the region of dust. This effect is not most conspicuous in the numerical plot (Fig. 2,b) calculated for the rather small dust size $a = 0.1 \text{ } \mu\text{m}$ and the ion density $n_{i0} = 1.024 \times 10^7 \text{ cm}^{-3}$. The attenuation of the ion flux in the vicinity of the shock front (as the shock passes through the region of the dust) calculated numerically for the same data as Fig. 2,b is only about seven per cent. Numerical analysis shows that the decrease in the shock amplitude and the attenuation of the ion flux manifest themselves stronger with increase in the dust size and the ion density.

The initial perturbation evolves in such a way that its front velocity V_p becomes nearly constant about 1 ms after it starts propagating through the background plasma. Fig. 3 shows the dependence of the perturbation front velocity (normalized to its value in the absence of dust, $\epsilon = 0$) on the parameter ϵZ_{d0} . For comparison, we also plot the experimental points (crosses) taken from Fig. 5 in [11]. The calculated results are represented by closed circles. The agreement between theory and experiment is quite good.

Thus, the ionization source model [18, 19] makes it possible to describe all the main experimental results on dust ion-acoustic shock waves.

2. Dissipative Processes

In the previous Section, we have presented the results of the theoretical modeling of dust ion-acoustic shocks with the aid of the ionization source model [18, 19] which is based on the hydrodynamical approach. Since dissipation is one of the processes that play a key role in the formation and propagation of dust ion-acoustic shocks, the hydrodynamic approach to describing these structures is valid only if dissipative processes that are taken into account in the hydrodynamic equations turn out to be more important than the Landau damping. Hence, it is important to classify dissipative processes and determine the ranges of plasma parameters, in which some particular processes dominate.

To evaluate the role of different dissipative processes in the propagation of nonlinear dust ion-acoustic perturbations, we derive an expression for the kinetic damping rate of ion-acoustic waves on the basis of a

purely kinetic approach to describing a complex plasma. The new expression for the kinetic damping rate in the case $\omega_{\mathbf{k}}^s \gg \nu_q$ is [21, 22]

$$\gamma_{\mathbf{k}}^L = \gamma_{\mathbf{k}}^{L,R} + \gamma_{\mathbf{k}}^{L,q}, \quad (2)$$

where

$$\gamma_{\mathbf{k}}^{L,R} \approx -\sqrt{\frac{\pi m_e n_{i0}}{8 m_i n_{e0}}} \frac{\omega_{\mathbf{k}}^s}{(1 + |\mathbf{k}|^2 \lambda_{De}^2)^{3/2}} \left(1 + \frac{n_{i0}}{n_{e0}} \sqrt{\frac{T_e^3}{T_i^3}} \sqrt{\frac{m_i}{m_e}} \exp \left[-\frac{T_e n_{i0}}{2 T_i n_{e0} (1 + |\mathbf{k}|^2 \lambda_{De}^2)} \right] \right), \quad (3)$$

$$\gamma_{\mathbf{k}}^{L,q} = -\nu_q \sqrt{\frac{\pi Z_{d0} d}{2}} \frac{(t + z_0)}{z_0 (1 + t + z_0) (1 + |\mathbf{k}|^2 \lambda_{De}^2)}, \quad (4)$$

m_e is the electron mass, $\lambda_{De} = \sqrt{T_e / 4\pi n_{e0} e^2}$ is the electron Debye length, \mathbf{k} is a wave number, $d = n_{d0} / n_{e0}$, $t = T_i / T_e$, and

$$\omega_{\mathbf{k}}^s \approx \frac{|\mathbf{k}| c_s \sqrt{n_{i0} / n_{e0}}}{\sqrt{1 + |\mathbf{k}|^2 \lambda_{De}^2}} \quad (5)$$

is the linear dispersion relation for dust ion-acoustic waves.

The first term $\gamma_{\mathbf{k}}^{L,R}$ on the right-hand side of relationship (2) describes the ordinary Landau damping on electrons and ions, and the second term $\gamma_{\mathbf{k}}^{L,q}$ describes the damping due to the interaction of electrons and ions with dust grains. The rates of these two damping processes are both referred to as the kinetic damping rate. The introduction of the common term is justified because, in a complex plasma, these processes are inseparable.

We emphasize that there are other approaches to describing the Landau damping of dust ion-acoustic waves (see [23]). In [23], only the first term $\gamma_{\mathbf{k}}^{L,R}$ in the kinetic damping rate (2) was taken into account. However, in some situations typical of present-day experiments with complex plasmas, the second term $\gamma_{\mathbf{k}}^{L,q}$ predominates over the first term. In fact, for the data of the experiments on dust ion-acoustic shocks in a Q-machine device, cesium vapor plasma with $T_e = T_i = 0.2$ eV, $a = 0.1$ μm , and the characteristic wave vector $|\mathbf{k}| \sim 2\pi / \Delta\xi \sim \nu_q / M c_s$ corresponding to the characteristic width (1) of the front of the shock wave associated with anomalous dissipation, the second term (with ν_q) in relationship (2) is larger than the first term under the condition $\epsilon Z_{d0} > 0.6$. To obtain this condition, we take into account the dependence of the Mach number M on ϵZ_{d0} (see Fig. 3). A dust ion-acoustic shock (front steepening) is observed in a Q-machine device when the

condition $\epsilon Z_{d0} > 0.6$ is satisfied. We thus arrive at the conclusion that the dust grain charging processes can substantially modify the rate of kinetic damping of dust ion-acoustic perturbations; moreover, in many situations, it is these charging processes that dominate the kinetic damping mechanism.

An analysis of the dispersion properties of ion-acoustic waves on the basis of the hydrodynamic ionization source model [18, 19] yields the following expression for the damping rate [21]:

$$\gamma_{\mathbf{k}} \approx -\Gamma \equiv -\frac{\nu_{\text{ch}} + \tilde{\nu}}{2}. \quad (6)$$

Here, ν_{ch} is the rate of absorption of ions by dust grains and $\tilde{\nu}$ is the rate, at which the ions lose their momentum as a result of their absorption on the grain surfaces and their Coulomb collisions with dust grains:

$$\nu_{\text{ch}} = \nu_q \frac{Z_{d0} d}{1 + Z_{d0} d} \frac{(t + z_0)}{z_0 (1 + t + z_0)}, \quad (7)$$

$$\tilde{\nu} = \nu_q \frac{Z_{d0} d}{(1 + Z_{d0} d) z_0 (1 + t + z_0)} \left(z_0 + \frac{4t}{3} + \frac{2z_0^2}{3t} \Lambda \right), \quad (8)$$

$\Lambda = \ln(\lambda_{Di} / \max\{a, b\})$ is the Coulomb logarithm; $\lambda_{Di} = \omega_{pi} / v_{Ti}$ is the ion Debye radius; and $b = Z_{d0} e^2 / T_i$. Note that expressions (7) and (8) are valid in the range $v_i / c_s < 1$, where v_i is the ion velocity.

A simple criterion for determining whether the above hydrodynamic model is applicable to nonlinear dust ion-acoustic structures is the condition $\Gamma > \gamma_{\mathbf{k}}^L$. The validity of this condition means that the dissipative processes that are taken into account in the hydrodynamic equations are more important than the kinetic damping. For cesium vapor plasma with $T_e = T_i = 0.2$ eV, $a = 0.1$ μm , $n_{i0} = 1.024 \times 10^7$ cm^{-3} , and the characteristic wave vector $|\mathbf{k}| \sim 2\pi / \Delta\xi \sim \nu_q / M c_s$, the condition $\Gamma > \gamma_{\mathbf{k}}^L$ is valid if $\epsilon Z_{d0} > 0.07$. Thus, for a wide range of the plasma and dust grain parameters in a Q-machine device, the hydrodynamic ionization source model is applicable for the description of the ion-acoustic nonlinear structures.

For $T_e \sim T_i$, the Landau damping is the most significant dissipation process for small ϵZ_{d0} (in our case, for $\epsilon Z_{d0} \leq 0.07$). The significant role of the Landau damping in this case means that it can make a contribution to a spreading out of the pulse as it propagates down the plasma column. The increase in the parameter ϵZ_{d0} leads to the diminution of the role of the Landau damping, while the processes of the charging of dust grains, of the absorption of ions by grains, and of the transfer of the ion momentum to grains become more important.

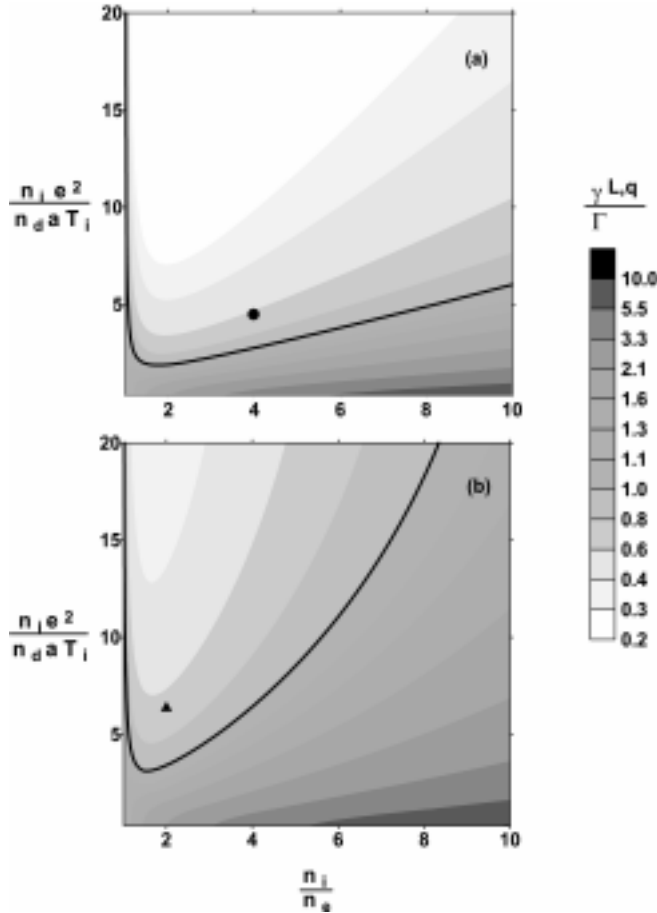


Fig. 4. Relief of the ratio $\gamma_k^{L,q}/\Gamma$ on the plane $(n_i e^2/n_d a T_i, n_i/n_e)$ for the plasma parameters (a) in the experiments of [11] ($T_e = T_i = 0.2$ eV, $n_i = 1.024 \times 10^7$ cm $^{-3}$, Cs $^+$ ions, $a = 0.1$ μ m) and (b) in the experiments of [10, 12] ($T_e = 1.5$ eV, $T_i < 0.1$ eV, $n_i = 2.3 \times 10^8$ cm $^{-3}$, Ar $^+$ ions, $a = 4.4$ μ m). The closed circle in plot (a) corresponds to $\epsilon Z_{d0} = 0.75$ and to the plasma parameters in the experiments of [11]. The closed triangle in plot (b) corresponds to $\epsilon Z_{d0} = 0.5$ and to the plasma parameters in the experiments of [10, 12]. The heavy curves correspond to $\gamma_k^{L,q} = \Gamma$

Since $\gamma_k^{L,q}$ in the kinetic description and Γ in the hydrodynamic description are related to the anomalous dissipation caused by the interaction of plasma particles with dust grains, i.e. they have the same origin, it is of interested to compare these rates.

Figs. 4 and 5 present the relief of the ratio $\gamma_k^{L,q}/\Gamma$ for the parameters of complex plasmas in the experiments in a Q-machine device, a double plasma device, and devices based on glow discharges and on high-frequency discharges. Fig. 4,a corresponds to the experimental conditions of [11]. The closed circle in Fig. 4,a corresponds to $\epsilon Z_{d0} = 0.75$. Figure 3,b was drawn

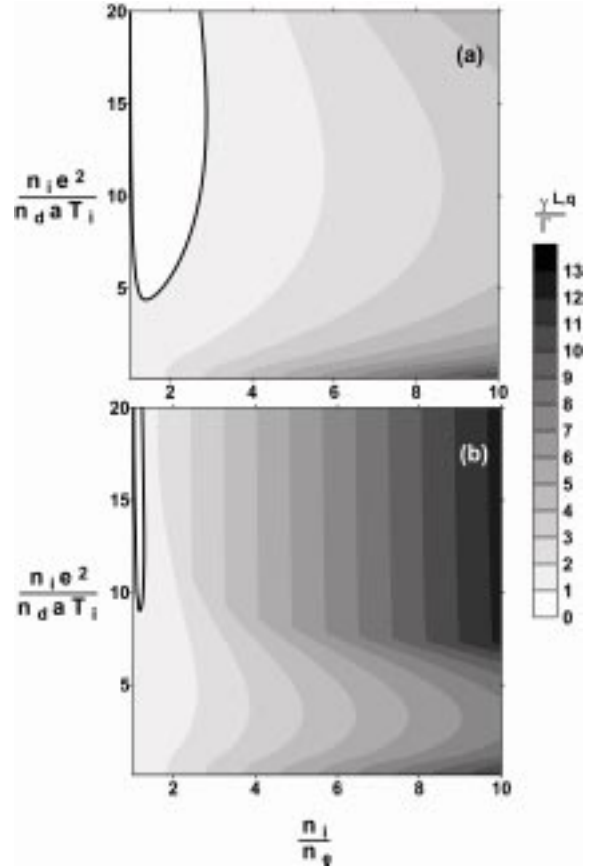


Fig. 5. Relief of the ratio $\gamma_k^{L,q}/\Gamma$ on the plane $(n_i e^2/n_d a T_i, n_i/n_e)$ for the plasma parameters (a) in the experiments of [17] ($T_e \approx 1$ eV, $T_i \approx 0.03$ eV, $n_i = 2 \times 10^9$ cm $^{-3}$, Ar $^+$ ions, $a = 3.4$ μ m) and (b) in the experiments of [24] ($T_e \approx 3$ eV, $T_i \approx 0.03$ eV, $n_e \approx 10^9$ cm $^{-3}$, Ne $^+$ ions, $a \approx 4$ μ m). The heavy curves correspond to $\gamma_k^{L,q} = \Gamma$

for the experimental conditions of [10]. The closed triangle in Fig. 3,b corresponds to $\epsilon Z_{d0} = 0.5$.

We emphasize that the analogous experimental parameters were used in [12]. It can be seen that the experimental parameters of [10–12] satisfy the inequality $\gamma_k^{L,q}/\Gamma < 1$. This indicates that the ionization source model is applicable to nonlinear dust ion-acoustic structures in a double plasma device and a Q-machine device. Fig. 5,a refers to the plasma parameters of experiments carried out on the board of the International Space Station [17]. Fig. 5,b was obtained for the plasma parameters in experiments with glow discharges [24]. We can see that, for $n_i/n_e = 1/(1 - \epsilon Z_{d0}) > 3$ in experiments [17] and for $n_i/n_e = 1/(1 - \epsilon Z_{d0}) > 1$ in the experiments of [24], the ratio $\gamma_k^{L,q}/\Gamma$ is always larger

than unity. This means that, over fairly wide ranges of the dust grain parameters, dust ion-acoustic structures in typical experiments carried out with complex plasmas on devices based on glow and rf discharges should be described in terms of kinetic theory. Thus, the condition $\gamma_{\mathbf{k}}^{L,q}/\Gamma > 1$ serves as a criterion for determining whether or not the kinetic approach is applicable to nonlinear dust ion-acoustic structures observed in experiments.

The dissipation related to the processes of momentum loss by ions as a result of their absorption on the grain surfaces and their Coulomb collisions with the grains forbids the existence of stationary shocks or solitons. There is no external source of ion momentum which is able to compensate for this momentum loss. This statement is valid independently whether we use the hydrodynamic or kinetic approach to nonlinear dust ion-acoustic waves. In the dust ion-acoustic nonstationary shocks, a balance between nonlinearity and dissipation is possible in the vicinity of their front, which results in the formation of a shock front during the time $\tau \sim \nu_q^{-1}$ much shorter than the characteristic time of shock propagation. But the amplitude of such shocks decreases.

In conclusion of this Section, we note that Nakamura et al. [10] attempted to describe their experimental results on the basis of the Korteweg—de Vries—Burgers (KdVB) equation with the dissipative viscosity coefficient proportional to the ion-grain collision rate (see also [25, 26]). The correctness of the use of the viscosity concept for the description of dust ion-acoustic shocks was analyzed in [27]. It was shown that the viscosity concept can not be introduced to analyze the observations on dust ion-acoustic shocks: the viscosity should be taken to be zero.

3. Dust Ion-Acoustic Solitons

Here, we describe briefly the main results of the investigation of the dust ion-acoustic solitons in complex plasmas [9]. The anomalous dissipation caused by the charging processes means that the existence of completely steady-state nonlinear structures is impossible. In reality, this note is true for any real system. However, in complex plasmas it leads to qualitatively new results which are related, in particular, to the necessity to take into account the effect of adiabatically trapped electrons. The main results of the investigation [9] are the following:

(1) The properties of the compressive solitons with trapped electrons are very different from those with not trapped those (Boltzmann electrons). In particular, the

maximum possible amplitude of a soliton with trapped electrons is much larger than that of a “Boltzmann” soliton, while the region of allowable Mach numbers for the former is much wider than for the latter. This shows the principal possibility to study experimentally the role of trapped electrons in the soliton formation.

(2) The evolution of the initial perturbation in the form of a steady-state compressive soliton with trapped electrons occurs in the following manner. The soliton is damped due to the dissipation originating from the dust particle charging processes. The speed of the perturbation decreases. However, at any time, the form of the evolving perturbation is similar to that of the steady-state compressive soliton with trapped electrons corresponding to the Mach number at this moment of time.

(3) After the interaction of two damped solitons, each perturbation has the form which is close to that of the same soliton perturbation propagating individually from the beginning (not subjected to the interaction). This property is inherent in solitons. Thus, there is a possibility of the existence of the dust ion acoustic compressive solitons which are damped and slowed down, but their form corresponds to the soliton one for the running value of their speed. They can be called as “weakly dissipative solitons”.

4. Active Experiments, Natural Phenomena, and Applications

Here, we present some possibilities of observation of the dust ion-acoustic shocks and some applications where their physics can be important.

(1) The idea of the formation of shocks related to dust charging in active rocket experiments, which use the scheme of the experiments Fluxus-1 and -2 [28, 29] and involve the release of some gaseous substance in the near-Earth space, was forwarded in [30]. The source for the charged particle release in the ionosphere in these experiments is a generator of high-speed plasma jets. The shock wave front is associated with the fore (border)-part of the jet propagating in the ionosphere plasma. Macroparticles (dust) appear as a result of the condensation. Drops are charged due to their interaction with the ambient plasma and the photoelectric effect. The optimum speeds of the jet are 10 km/s. The optimum altitudes for such experiments are 500–600 km. The scheme of the active experiment is given in Fig. 6. The active experiments, where the shocks in charge-varying dusty plasmas can be observed, can be

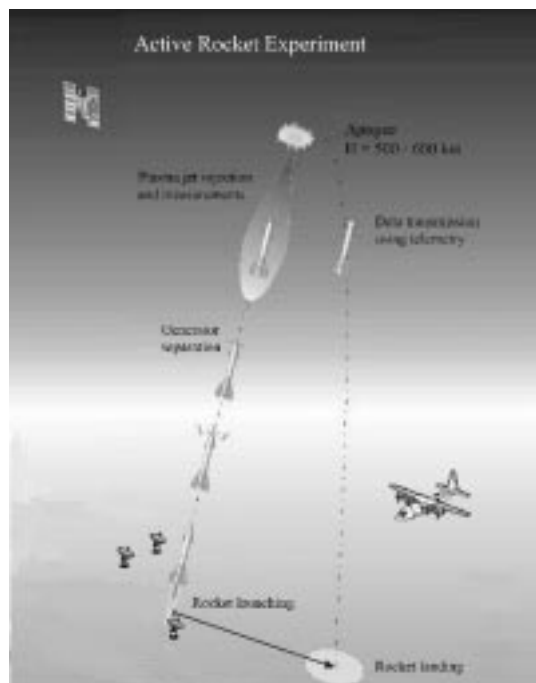


Fig. 6. The scheme of the active rocket experiment, which involves the release of some gaseous substance in near-Earth space

helpful to model different physical phenomena occurring in nature, e.g., in the process of a large meteoroid impact with the Moon surface [31]. The evolution of the impact plume can lead to the formation of a shock wave structure associated with the appearance of charged microparticles which are created in the process of condensation of the substance of the vapor plume as well as are thrown from the crater and the surrounding regolith layer.

(2) The presence of dust in cometary coma can modify the shock wave formed as a result of the interaction of the solar wind with a comet [32]. The outer shock wave (bow shock) can be considered as a dust ion-acoustic shock wave, because it is formed as a result of the interaction of cometary ions with solar-wind protons. For the dust densities $n_d > 10^6 \text{ cm}^{-3}$ near the comet nucleus, charged dust particles influence drastically the structure of the bow shock front. Its width is in accordance with the theory of shocks related to dust particle charging.

(3) The dust ion-acoustic shocks also may find significant technological applications in, e.g., the so-called hypersonic aerodynamics. The main difficulties of hypersonic flight in the atmosphere are associated with the generation of shock waves, which leads to heavy mechanical and thermal loads on the structural

components of an aircraft, considerably increases the resisting forces, and lowers the engine efficiency. Usually, these negative effects are reduced through an optimum streamlining of the aircraft. However, a more promising possibility seems to be changing the properties of the air surrounding the aircraft. In this way, the negative effects may be lessened by modifying the mechanisms for the formation and propagation of shock waves by plasma methods (such as a local heating of air around the aircraft). However, the dust (aerosol) that is produced due to the condensation from the surrounding air can, in turn, modify the behavior of the shock-wave structures. That is why the understanding of the dissipation mechanisms in shock-wave structures is of key importance in such situations.

5. Melting Dust Acoustic Shock in a 2D Complex Plasma

Dust ion-acoustic nonlinear structures correspond to the situation when one can neglect the motion of dust grains. Thus, for such structures, it is not very important whether the complex plasma is in a weakly or strongly coupled state. The opposite situation takes place in the case of dust acoustic nonlinear structures. A significant example is the shock melting in a two-dimensional strongly coupled complex plasma.

The experiments on shocks in a laboratory two-dimensional complex plasma which suggest the melting transition from "flat" dusty plasma crystals to the liquid (and possibly gaseous) phase were performed [15] in a setup using a capacitively coupled rf discharge. A short negative pulse (-100 V , 50 ms applied to a wire for 0.07 s) pushed the dust particles away breaking the lattice above the wire and creating a pulsed one-dimensional compressional disturbance propagating horizontally perpendicular to the wire. The disturbance propagated to the other end of the crystal and melted it from the excitation edge to about the middle of the field of view. A time interval of about 1 min allowed the lattice to come to an equilibrium between the experimental runs and to recrystallize. The disturbance can be treated as a shock wave because:

(1) The kinetic temperature of dust grains and the defect fraction have a jump at the shock front, there is the density compression;

(2) There is the mass transfer via the shock front. The mass transfer is described well by the first Hugoniot relationship;

(3) The width of the shock front is determined by several mean free paths of dust grains in the region of

the shock front. This is related to the fact that grains are in the “collisional regime” in this region. The observed shock is related to the melting of the plasma crystal.

The mechanism of the formation of the disordered state behind the shock front is the increase in the dust grain temperature (up to 300 eV) behind the front. For such a temperature the Coulomb coupling parameter becomes of the order of 1. This is a nonequilibrium phase transition [33] different from both straightforward first-order and classical second-order transitions.

6. Dust Acoustic Nonlinear Structures in Weakly Coupled Complex Plasmas

The above results [15] are referred to the strongly coupled complex plasma state. Dust acoustic nonlinear structures were observed also in the weakly coupled complex plasma state, in a dc glow-discharge plasma [16]. The structure consisted of two compressional regions separated by a rarefaction and propagated with the velocity of the order of the dust acoustic velocity. One of the compressions had a higher amplitude and, before it, the weaker one was running. After the passing of the stronger compression, the dust returned to the unperturbed configuration. The wave is supposed [16] to be instability-driven. Supersonic dust grains moving in the inverse direction with respect to the wave propagation were observed in the rarefaction area.

Another example of dust acoustic nonlinear waves is localized structures of nanosize charged dust grains in the Earth’s middle atmosphere [34] which exhibits layered phenomena known as noctilucent clouds and polar mesosphere summer echoes at altitudes of 80–95 km. These structures are believed to be associated with the presence of large quantities of charged dust or aerosol particles. Localized dust acoustic structures can exist in the mesosphere at altitudes of 80–95 km. Their main properties are determined mainly by the sign of the local dust charge. Dust grains consisting of pure ice have nanoscale sizes and are negatively charged. Impurities containing dust grains can have a surface work function less than the threshold for photoemission due to the solar irradiation, so that they can become positively charged. Dust acoustic structures containing positive grains appear as electron-density humps and ion-density dips, and those with negative grains appear as electron-density dips and ion-density humps. As a rule, structures with electron humps are more intense than those with electron dips. These results seem to agree with experimental observations. Such properties of the localized structures can help in the determination

of the sign and composition of mesospheric dust grains. In general, knowledge of the nonlinear structures is also useful for understanding the origin, behaviour, and effect on the noctilucent clouds and polar mesosphere summer echoes on the mesosphere and its relation to the other regions of the Earth’s atmosphere.

Summary

Thus, the anomalous dissipation originating from the charging processes results in a possibility of the existence of a new kind of shocks. The theoretical ionization source model allows us to describe all the main results on the dust ion-acoustic shocks obtained in the laboratory experiments. There is a possibility of the existence of the dissipative dust ion-acoustic solitons. The dust ion acoustic nonlinear structures are important in different real and artificial objects of geophysical and space plasmas. Dust acoustic nonlinear structures can propagate both in strongly and weakly coupled complex plasma. In strongly coupled complex plasmas, the dust acoustic shock propagation can lead to the melting of the plasma crystal. This is a nonequilibrium phase transition different from both straightforward first-order and classical second-order transitions.

This work was supported in part by INTAS (grant No. 01-0391) and the Russian Foundation for Basic Research (project No. 03-02-16664-a). One of the authors (S.I.P.) would like to thank the Russian Ministry of Education and Science and Deutsche Akademische Austausch Dienst (DAAD) for a fellowship within the Program “Mikhail Lomonosov”.

1. *Dusty Plasmas* / Ed. by A. Bouchoule. — Chichester: Wiley, 1999.
2. *Chu J.H., Lin I.* //Phys. Rev. Lett. **72** (1994) 4009.
3. *Thomas H., Morfill G.E.* //Nature **379** (1996) 806.
4. *Tsytoich V.N.* //Physics-Uspekhi **40** (1997) 53 [Uspekhi Fiz. Nauk **167**, 57 (1997)].
5. *Vladimirov S.V., Ostrikov K.* //Phys. Repts. **393**(2004) 175.
6. *Fortov V.E., Khrapak A.G., Khrapak S.A., Molotkov V.I., Petrov O.F.* //Physics-Uspekhi **47** (2004) 447 [Usp. Fiz. Nauk **174** (2004) 495].
7. *Tsytoich V.N., Havnes O.* //Comments Plasma Phys. Control. Fusion **15** (1993) 267.
8. *Popel S.I., Yu M.Y., Tsytoich V.N.* //Phys. Plasmas **3** (1996) 4313.
9. *Popel S.I., Golub’ A.P., Losseva T.V. et al.* //Phys. Rev. E **67** (2003) 056402.
10. *Nakamura Y., Bailung H., Shukla P.K.* //Phys. Rev. Lett. **83** (1999) 1602.

11. Luo Q.-Z., D'Angelo N., Merlino R.L. //Phys. Plasmas **6** (1999) 3455.
12. Nakamura Y., Sarma A. //Phys. Plasmas **8** (2001) 3921.
13. Samsonov D., Goree J., Ma Z.W. et al. //Phys. Rev. Lett. **83** (1999) 3649.
14. Samsonov D., Goree J., Thomas H.M., Morfill G.E. //Phys. Rev. E **61** (2000) 5557.
15. Samsonov D., Zhdanov S.K., Quinn R.A. et al. //Phys. Rev. Lett. **92** (2004) 255004.
16. Fortov V.E., Petrov O.F., Molotkov V.I. et al. //Phys. Rev. E **69** (2004) 016402.
17. Samsonov D., Morfill G., Thomas H. et al. //Ibid. **67** (2003) 036404.
18. Popel S.I., Golub' A.P., Losseva T.V., Bingham R. //JETP Lett. **73** (2001) 223 [Pis'ma Zh. Eksp. Teor. Fiz. **73** (2001) 258].
19. Popel S.I., Golub' A.P., Losseva T.A. et al. //Phys. Plasmas **8** (2001) 1497.
20. Nakamura Y., Bailung H. //Rev. Sci. Instrum. **70**(1999) 2345.
21. Popel S.I., Andreev S.N., Gisko A.A. et al. //Plasma Phys. Rep. **30** (2004) 284 [Fiz. Plazmy **30** (2004) 314].
22. Popel S.I., Losseva T.V., Golub' A.P. et al. (to be published).
23. Rosenberg M. //Planet. Space Sci. **41** (1993) 229.
24. Nefedov A.P., Petrov O.F., Fortov V.E. //Physics-Uspekhi **40** (1997) 1163 [Uspekhi Fiz. Nauk **167** (1997) 1215].
25. Shukla P.K. //Phys. Plasmas **7** (2000) 1044.
26. Ghosh S., Sarkar S., Khan M., Gupta M.R. //Ibid. **9** (2002) 378.
27. Thomas H., Morfill G., Tsytovich V.N. //Plasma Phys. Repts. **29** (2003) 895 [Fiz. Plazmy **29** (2003) 963].
28. Gavrilov B.G., Podgorny A.I., Podgorny I.M. et al. //Geophys. Res. Lett. **26** (1999) 1549.
29. Erlandson R.E., Swaminathan P.K., Meng C.-I. et al. //Ibid. (1999) 1553.
30. Popel S.I., Tsytovich V.N. //Astrophys. Space Sci. **264** (1999) 219.
31. Nemtchinov I.V., Shuvalov V.V., Artemieva N.A. et al. //Intern. J. Impact Eng. **27** (2002) 521.
32. Popel S.I., Gisko A.A., Losseva T.V., Vladimirov S.V. //30th EPS Conf. on Controlled Fusion and Plasma Phys.: Abstr. **27A** (2003) 4.125.
33. Klimontovich Yu.L. Statistical Theory of Open Systems. — Dordrecht: Kluwer, 1995. — Vol. I.
34. Kopnin S.I., Kosarev I.N., Popel S.I., Yu M.Y. // Planet. Space Sci. **52** (2004) 1187.

НЕЛІНІЙНІ ХВИЛІ У КОМПЛЕКСНІЙ ПЛАЗМІ:
ТЕОРІЯ І ЕКСПЕРИМЕНТ

С.І. Попель, Г.Е. Морфілл

Резюме

Розглянуто теоретичні й експериментальні результати досліджень структури нелінійної хвилі у комплексній запорошеній плазмі. Показано, що модель гідродинамічної іонізації застосовна до пилових іонно-звукових нелінійних хвиль у газорозрядній і двокомпонентній плазмі. Досліджено найважливіші дисипативні процеси, відповідальні за утворення пилових іонно-звукових нелінійних хвиль. Серед цих процесів аномальна дисипація, що відповідає процесові заряджання порошинок пилу, поглинання та розсіяння іонів порошинами, а також кінетичне затухання, в тому числі затухання Ландау. Обговорено можливість спостереження пологої іонно-звукової ударної хвилі у ракетному експерименті в іоносфері Землі, а також застосування таких ударних хвиль в природних явищах і технологіях. Пиловозвукові нелінійні хвилі описані для випадків слабо- і сильновзаємодіючої комплексної плазми.